

2D and 3D numerical analysis on strut responses due to one-strut failure

Wengang Zhang^{*1,2,3}, Runhong Zhang^{2a}, Yinrong Fu^{2b}, A.T.C. Goh^{4c} and Fan Zhang^{5d}

¹National Joint Engineering Research Center of Geohazards Prevention in the Reservoir Areas, Chongqing University, Chongqing, 400045, China

²School of Civil Engineering, Chongqing University, Chongqing, 400045, China

³Key Laboratory of Rock Mechanics in Hydraulic Structural Engineering, Ministry of Education, Wuhan University, 430072, China

⁴School of Civil and Environmental Engineering, Nanyang Technological University, 639798, Singapore

⁵IIIBIT-Sydney, Federation University, NSW 2000, Australia

(Received October 15, 2016, Revised October 30, 2017, Accepted January 6, 2018)

Abstract. In deep braced excavations, struts and walers play an essential role in the whole supporting system. For multi-level strut systems, accidental strut failure is possible. Once a single strut fails, it is possible for the loads carried from the previous failed strut to be transferred to the adjacent struts and therefore cause one or more struts to fail. Consequently, progressive collapse may occur and cause the whole excavation system to fail. One of the reasons for the Nicoll Highway Collapse was attributed to the failure of the struts and walers. Consequently, for the design of braced excavation systems in Singapore, one of the requirements by the building authorities is to perform one-strut failure analyses, in order to ensure that there is no progressive collapse when one strut was damaged due to a construction accident. Therefore, plane strain 2D and three-dimensional (3D) finite element analyses of one-strut failure of the braced excavation system were carried out in this study to investigate the effects of one-strut failure on the adjacent struts.

Keywords: three-dimensional; braced excavation; one-strut failure; load transfer percentage; load increase percentage; finite element

1. Introduction

In Singapore, braced retaining wall systems are commonly used to construct cut and cover tunnels/stations for Mass Rapid Transit (MRT) projects as well as for deep basements for shopping malls. The sides of the excavation are normally supported by concrete diaphragm walls or secant bored pile walls with two or more levels of struts. The purpose of the excavation support system is to provide rigid lateral support for soil surrounding the excavation and to limit the movement of the surrounding soils. The method presented by Peck (1969) for specifying apparent lateral earth pressures forms the basis of the design of the excavation support systems and the determination of the loads on the bracing systems. However, the limitation of Peck's method have been highlighted by Liao and Neff (1990), and various enhancements to the method have been proposed by Liao and Neff (1990), Chang and Wong (1997), and Twine and Roscoe (1997). The mechanisms controlling the development of lateral earth pressure around a braced excavation in a deep deposit of soft clay has been presented by Hashash and Whittle (2002).

One concern in the design of these cut and cover excavation projects is the consequence of the failure of one or two struts (due to accidental damage during construction) in the bracing system and whether it would lead to progressive failure and eventual total collapse of the bracing systems and the surrounding grounds (Endicott 2013, Saleem 2015, Goh *et al.* 2017, Xiang *et al.* 2018, and Zhang *et al.* 2018). One of the main reasons for excavation work collapse of Hangzhou Xianghu subway station causing 21 deaths lies in the poor connection between the strut and Walers, which triggered the subsequent progressive failure.

The 30m deep excavation collapse adjacent to the Nicoll Highway in Singapore is also partially due to the failure or poor connections of the strut. Consequently, the focus of this paper is on one-strut failure analyses, to study how the loads from the failed strut are transferred to the adjacent struts and support system.

To date, only limited studies have been carried out to examine this aspect in retaining walls supported by multi-levels of anchors/struts. One widely reported field study was carried out at four sites in Sweden and were described in Stille (1976), and Stille and Broms (1976). Stille (1976) reported that at the four sites, the maximum change of the anchor load expressed as a percentage of the initial load of the failed anchor was 35% for walls with two or more rows of anchors. The field study indicated that the increase in the loads of the adjacent anchors was of the same order of magnitude in the horizontal and vertical directions. As the associated wall movements were small, it was concluded that the transfer of load to the adjacent anchors was not through the arching of the soil behind the wall, but through

*Corresponding author, Professor
E-mail: cheungwg@126.com

^aPh.D. Student

^bGraduate Student

^cProfessor

^dPh.D. Student

the wall and wale members. The numerical analysis performed by Goh and Wong (2009) indicated that the failure of one or two struts due to an accident would not result in detrimental failure of the entire excavation system, provided the struts have been adequately against compression failure. Low *et al.* (2012) presented the design approach and consideration for the temporary removable ground anchor using TR26:2010, based on a Singapore mass rapid transit (MRT) case. Pong *et al.* (2012) proposed a simplified procedure to rationally idealise the one-strut failure problem from a 3D analysis to a 2D plain strain analysis.

Unfortunately, in the case of braced strut systems, there is no reported case history detailing the load transfer mechanism due to one-strut failure. Since struts provide passive resistance to wall movement, while anchors rely on stresses in the ground being mobilized to retain the wall, it may not be realistic to compare the redistribution of forces for anchors and struts. In Singapore, part of the design requirement requires that the braced retaining wall system to be structurally safe, robust and has sufficient redundancy to avoid catastrophic collapse due to one-strut failure. In the conventional approach for one-strut failure using 2D analysis, the entire level of the failing strut is removed and thus the forces can only be distributed vertically. This generally leads to a more conservative design with heavier strut sections. Thus, 3D analysis of one-strut failure is essential to provide more realistic understanding of the force/stress transfer behaviour of the braced excavation system. This paper describes the use of 2D and 3D finite element analyses to assess the impact of the failure of one strut on the remaining struts.

2. Numerical schemes

For the numerical simulations carried out in this study, geotechnical software PLAXIS 2D (V9.0) and PLAXIS 3D Foundation were used (Brinkgreve *et al.* 2011). Fig. 1 shows a typical cross-section and plan view for the cases considered. The parameters shown in the figure include: L =excavation length, B =excavation width, D =wall penetration depth, T =clay thickness below the final excavation level (FEL), S_H =horizontal strut spacing, S_V =vertical strut spacing and H_e =depth of final excavation. Vertical retaining walls along the excavation boundary were installed together with a five-level strut and waling system.

The compositions of clay layers were varied for the different cases studied. For 2D analyses, a half mesh was used due to geometrical symmetry. A very fine mesh size consisting of 10,390 nodes and 1,254 15-node triangular elements, was used for 2D analysis to improve the accuracy of FE calculations. For 3D analyses, a medium mesh size in the horizontal direction and medium coarse mesh size in vertical direction were used to reach a balance between processing time and accuracy. For brevity, only a typical 3D half mesh is shown in Fig. 2, comprising of 15,679 nodes and 4,980 15-node wedge elements.

For the 2D simulations, fourth order 15-node triangular elements, which are considered to be very accurate

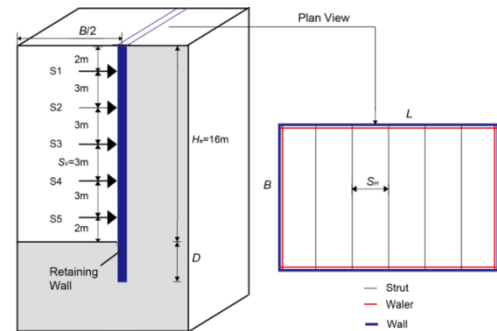


Fig. 1 Cross-section and plan view of the model for braced excavation

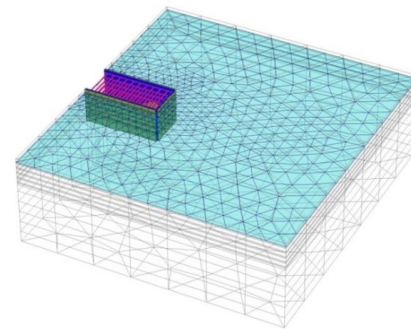


Fig. 2 3D half mesh of the excavation from PLAXIS 3D foundation

Table 1 Wall properties for 2D and 3D analyses

Parameters	Wall types			
	Flexible	Medium	Stiff	
Plane strain (2D) FE parameters				
	0.1	1.0	10	
System stiffness S	32	320	3200	
EI (kNm ² /m)	5.04E+04	5.04E+05	5.04E+06	
EA (kN/m)	3.427E+06	3.427E+07	3.427E+08	
Poisson's ratio ν	0	0	0	
Three-dimensional (3D) FE parameters				
Young's Modulus (kPa)	E_1	8.16E+06	8.16E+07	8.16E+08
	E_2	4.08E+05	4.08E+06	4.08E+07
	E_3	2.00E+08	2.00E+09	2.00E+10
Shear Modulus (kPa)	G_{12}	4.08E+05	4.08E+06	4.08E+07
	G_{13}	4.00E+05	4.00E+06	4.00E+07
	G_{23}	1.333E+06	1.333E+07	1.33E+08
Poisson's ratio	ν	0	0	0

elements, were used to model the soil while the interface elements have 5 integration points. In 3D PLAXIS, the interface elements have 9 point Gauss integration with three translational degrees of freedom for each node. This is described in greater detail in Van Langen (1991). For the 2D analysis, the retaining wall is simulated using 5-node elastic plate elements. The elastic behaviour is defined by the following parameters: EA: normal stiffness, EI: bending stiffness, ν : Poisson's ratio. For the 3D analysis, the wall is simulated using 8-node quadrilateral plate elements with six

degrees of freedom per node.

In this study, three different wall stiffness values were considered for each soil type, as listed in Table 1. Based on the approach adopted by Finno *et al.* (2007), the wall thickness of 0.42 m was set to an arbitrary (constant) value so that the moment of inertia I and area A were kept constant, and only the wall elastic modulus E was varied. A coefficient α was introduced to represent walls with different rigidities (Bryson and Zapata-Medina 2012). The baseline bending stiffness EI for the analysis is 5.04×10^5 kNm²/m, which refers to a wall of medium stiffness based on the databases of Long (2001) and Moorman (2004). Therefore, $\alpha=1$ for cases with this wall stiffness, while a smaller $\alpha=0.1$ represents flexible walls and larger α represents stiff walls. The system stiffness, S is defined as

$$S = \frac{EI}{\gamma_w h_{avg}^4} \quad (1)$$

where EI = wall stiffness, γ_w = unit weight of water, and h_{avg} = average vertical strut spacing

The struts were simulated using node-to-node anchor elements in 2D analysis. For 3D analysis, the struts and walers were modelled as beam elements, which have six degree of freedom per node. This is described in greater details in Brinkgreve *et al.* (2011). For the braced excavations in this paper, the struts were placed horizontally at a spacing of 4 or 5 meters (for different case studies) in two directions to form a frame net. The walings were used to connect the excavation wall and the struts. The material properties are tabulated in Table 2.

The boundary conditions for 2D and 3D cases were: 1) rollers at side boundaries to allow vertical displacements and 2) pinned at the base to restrain any movements. For both 2D and 3D cases, the lateral boundaries in the side directions were set at least 100 m away from the centre of the excavation to eliminate the influence of the boundary restraints on the ground movements. This ensures that the lateral boundaries are beyond the settlement influence zone (which is typically 2 times of the excavation depth) induced by the excavation as proposed by Hsieh and Ou (1998). In this study, the clay thickness below the final excavation level T is assumed as 32 m, which is regarded as fairly large. A typical staged construction simulation is shown in Table 3. The original ground water table was assumed to be 2 m below the ground surface in the retained soil. The water table inside the excavation was progressively lowered with the excavation of the soil during each phase.

A series of 2D and 3D analyses covering various cases of wall stiffness α , soil types, excavation geometries and different strut levels and locations using the Hardening Soil (HS) model were conducted. For brevity, only the main findings of the numerical results are presented in the following sections. For all the 2D and 3D cases, the height of wall H_w is fixed at 20 m, so the depth of wall penetration D decreases as H_e increases. Apart from slight differences with regard to the excavation depth H_e , identical construction procedures were applied as described in Table 3.

The properties of three different types of clays which were considered in this parametric study are similar to the

Table 2 Properties of waling system

Parameter	Struts	Walers	
Unit weight γ (kN/m ³)	78.5	78.5	
Cross section area A (m ²)	0.007367	0.008682	
Young's Modulus E (kPa)	2.1E8	2.1E8	
Moment of inertia (m ⁴)	I_3	5.073E-5	1.045E-4
	I_2	5.073E-5	3.668E-4
	I_{23}	0	0

Table 3 Typical construction sequence for 2D analysis

Phases	Construction details
Phase 1	Install the excavation wall
Phase 2	Reset displacement to zero, excavate to 3 m below ground surface
Phase 3	Install strut system at 2 m below ground surface
Phase 4	Excavate to 6 m below ground surface
Phase 5	Install strut system at 5 m below ground surface
Phase 6	Excavate to 9 m below ground surface
Phase 7	Install strut system at 8 m below ground surface
Phase 8	Excavate to 12 m below ground surface
Phase 9	Install strut system at 11 m below ground surface
Phase 10	Excavate to 15 m below ground surface
Phase 11	Install strut system at 14 m below ground surface
Phase 12	Excavate to 16 m below ground surface
Phase 13	Remove the chosen strut

Table 4 Input HS soil parameters of three clays

Parameter	Unit	A: Soft clay (Chicago clay)	B: Medium clay (Taipei silty clay)	C: Stiff clay (Gault clay)
$unsat$	kN/m ³	18.1	18.1	20
sat	kN/m ³	18.1	18.1	20
E_{50}^{ref}	kN/m ²	2350	6550	14847
E_{oed}^{ref}	kN/m ²	2350	6550	14847
E_{ur}^{ref}	kN/m ²	7050	19650	44540
c	kN/m ²	0.05	0.05	0.05
ϕ	°	24.1	29	33
Ψ	°	0	0	0
v_{ur}	[-]	0.2	0.2	0.2
p^{ref}	kN/m ²	100	100	100
m	[-]	1.0	1.0	1.0
K_{nc}^0	[-]	0.59	0.55	1.5
R_f	[-]	0.7	0.95	0.96
R_{inter} (interface friction)	[-]	1	1	1

properties assumed by Bryson and Zapata-Medina (2012) and are tabulated in Table 4. The soils are assumed to follow the Hardening Soil (HS) model. The three soil types are: soft clay, medium clay and stiff clay. The clays are real soils whose properties have been extensively reported in the literature. The properties of the soft clay with average $c_u=20$ kPa are based on the Upper Blodgett soft clay reported by Finno *et al.* (2002). The medium clay with average $c_u=45$ kPa are based on the Taipei silty clay found at the Taipei

National Enterprise Centre (TNEC) project (Ou *et al.* 1998). The Gault clay at Cambridge (Ng 1992, Ng and Yan 1998) with average $c_u=125$ kPa was used as the model for the stiff clay.

3. Numerical simulation results

In order to investigate the influence of the one-strut failure on the adjacent struts, the strut forces before and after strut failure are examined. By tabulating the load transfer percentage and load increase percentage, the influence of the strut failure can be demonstrated. Assume N_{pre} is the load on the strut before strut failure; N_{post} is the load on the strut after strut failure and N_{fail} is the load on the failed strut before failure. Then the load transfer and load increase percentage are defined as Eqs. (2) and (3), respectively.

$$\text{Load Transfer (\%)} = \frac{N_{post} - N_{pre}}{N_{fail}} \times 100\% \quad (2)$$

$$\text{Load Increase (\%)} = \frac{N_{post} - N_{pre}}{N_{pre}} \times 100\% \quad (3)$$

3.1 One-strut failure for soft clay: $H_e = 12$ m with 3-levels of struts

The load transfer and increase percentages from 2D analyses are tabulated in Table 5, and the 3D results are shown in Table 6 and 7. It is worth mentioning that for the top strut (S1), although the load increase percentage appears high (approximately 8 times of the original value), the actual magnitude of the change in the force in strut S1 is small, as the force in S1 is small prior to the one-strut failure. In addition, S1 goes into tension after the failure of the 3rd level strut S3 as a result of kick-out of the wall. The 2D results indicate that failure of S3 leads to considerable increase in the load for the 2nd level S2 strut. On the other hand, the 3D results indicate that the load of the failed strut is not only transferred vertically upward, but also to the adjacent horizontal and diagonal struts as shown in the figure, where larger arrows denote the larger magnitude of the transferred loads and the red circles denote the struts with more than 10% load increase after the one-strut failure. In addition, for the 3D analyses the magnitude of the load transfer and increase percentages are much smaller, up to approximately 20% for flexible walls and 50% for medium walls compared with the results from the 2D analyses. Therefore, compared to 3D results, the 2D analyses overestimate the possible consequence of the one-strut failure for soft clay, as it ignores the restraining effects of the adjacent horizontal struts.

3.2 One-strut failure for medium and stiff clays: $H_e = 16$ m with 5-levels of struts

The load transfer and load increase percentages of the one-strut failure from 2D analyses for medium and stiff walls are shown in Table 9. For medium clay, most of the

Table 5 Load transfer and increase percentages from 2D analyses for the one-strut failure of S3 (soft clay)

Struts	Load Transfer %		Load Increase %	
	$\alpha=0.1$	$\alpha=1.0$	$\alpha=0.1$	$\alpha=1.0$
S1	-37.7	-30.4	-932.6	179.0
S2	122.2	120.3	220.1	172.1
S3	Failed strut		Failed strut	

Table 6 Load transfer percentage from 3D analyses for the one-strut failure of S3 (soft clay, $L/B = 2.2$)

Struts	Load Transfer %				
	$x^* = -8$	$x = -4$	$x = 0$	$x = 4$	$x = 8$
soft clay, $\alpha = 0.1$					
S1	-0.1	-2.5	-9.2	-2.5	0.2
S2	-0.5	9.7	15.4	9.2	-2.2
S3	2.7	23.3	Failed strut	21.1	-0.1
soft clay, $\alpha = 1.0$					
S1	-5.7	-4.4	-3.3	-3.7	-3.0
S2	1.5	11.9	53.6	11.2	-0.7
S3	4.2	24.4	Failed strut	22.5	3.3

* x , horizontal distance away from the failed strut, in meters

Table 7 Load increase percentage from 3D analyses for the one-strut failure of S3 (soft clay, $L/B = 2.2$)

Struts	Load increase %				
	$x = -8$	$x = -4$	$x = 0$	$x = 4$	$x = 8$
soft clay, $\alpha = 0.1$					
S1	-6.7	-192.8	-793.3	-185.6	13.9
S2	-0.8	14.7	23.2	14.0	-3.4
S3	2.9	23.6	Failed strut	21.3	-0.1
soft clay, $\alpha = 1.0$					
S1	33.6	22.6	16.2	18.7	17.8
S2	1.5	11.8	52.8	11.1	-0.7
S3	3.2	20.4	Failed strut	18.7	2.8

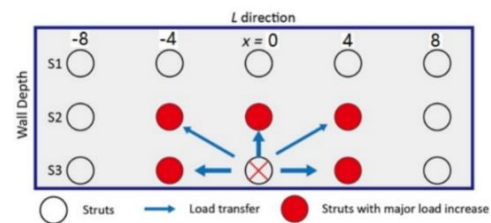


Fig. 3 Influence zone of the one-strut failure of S3 (soft clay)

load of the failed strut is transferred to the struts immediately above and below the failed strut, with approximately 30% to 50% of the load transferred to the upper strut and the remainder carried by the lower strut. For stiff clay, the failure of strut S3 leads to the force redistribution for the S2, S4 and S5 struts. The S2 and S4 struts each carry approximately 30% of the load of the failed strut, and S5 carries approximately 10% to 20%.

Table 8 Load transfer percentage from 2D analyses (medium and stiff clays)

Clay type	Struts	Load transfer (%)		
		$\alpha = 0.1$	$\alpha = 1.0$	$\alpha = 10$
Medium clay	S1	-0.9	-0.9	-0.4
	S2	-5.2	11.2	15.5
	S3	46.0	41.7	31.1
	S4	Strut failure		
	S5	53.4	47.1	46.3
Stiff clay	S1	-0.8	2.4	15.4
	S2	27.6	30.2	23.1
	S3	Strut failure		
	S4	29.3	29.5	22.1
	S5	10.8	11.9	14.6

Table 9 Load increase percentage from 2D analyses (medium and stiff clays)

Clay type	Struts	Load increase (%)		
		$\alpha = 0.1$	$\alpha = 1.0$	$\alpha = 10$
Medium clay	S1	-6.9	11.1	1.4
	S2	-10.4	21.7	35.5
	S3	63.3	54.0	31.2
	S4	Strut failure		
	S5	140.2	120.2	159.8
Stiff clay	S1	-1.5	4.6	20.4
	S2	29.1	32.4	23.9
	S3	Strut failure		
	S4	34.2	35.6	29.1

Table 10. Load transfer percentage from 3D analyses for the one-strut failure of S4 for medium clay ($L/B = 2.2$)

Struts	Load transfer %				
	$x = -8$	$x = -4$	$x = 0$	$x = 4$	$x = 8$
S1	-1.1	0.2	1.6	0.2	-1.0
S2	-0.3	3.1	7.9	3.2	-0.3
S3	0.5	5.5	15.3	5.5	0.5
S4	1.2	7.2	Failed strut	7.2	1.3
S5	2.8	9.0	19.5	9.0	2.7

Table 11 Load increase percentage from 3D analyses for the one-strut failure of S4 for medium clay ($L/B = 2.2$)

Struts	Load increase %				
	$x = -8$	$x = -4$	$x = 0$	$x = 4$	$x = 8$
S1	3.4	-1.0	-8.8	-1.2	4.3
S2	-0.8	8.2	20.6	8.2	-0.8
S3	0.6	6.5	18.0	6.7	0.6
S4	1.2	7.2	Failed strut	7.4	1.4
S5	9.4	29.9	65.0	30.4	9.8

Table 12 Load transfer percentage from 3D analyses for the one-strut failure of S4 for medium clay ($L/B = 3.4$)

Struts	Load transfer %				
	$x = -8$	$x = -4$	$x = 0$	$x = 4$	$x = 8$
S1	-0.3	0.8	2.0	0.5	-0.7
S2	-0.1	3.4	8.0	3.2	-0.2
S3	-0.1	5.3	15.1	5.4	0.4
S4	0.2	6.5	Failed strut	6.5	0.7
S5	1.4	7.5	17.9	7.4	1.5

Table 13 Load increase percentage from 3D analyses for the one-strut failure of S4 for medium clay ($L/B = 3.4$)

Struts	Load increase %				
	$x = -8$	$x = -4$	$x = 0$	$x = 4$	$x = 8$
S1	1.7	-4.5	-11.4	-3.2	4.4
S2	-0.3	7.9	18.3	7.4	-0.4
S3	-0.1	5.8	16.5	5.8	0.4
S4	0.2	6.5	Failed strut	6.5	0.7
S5	4.7	26.0	62.1	25.8	5.1

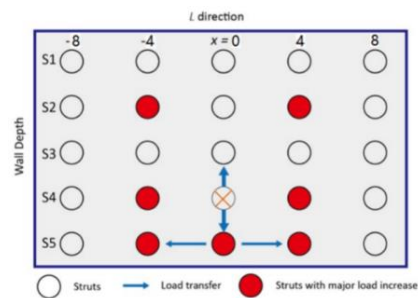


Fig. 4 Influence zone of the failure of S4 (medium clay)

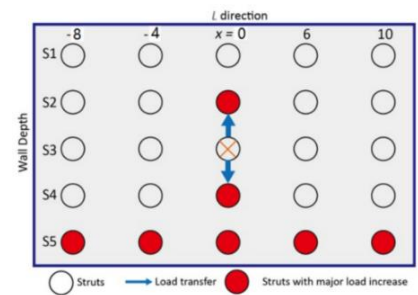


Fig. 5 Influence zone of the failure of S3 (stiff clay)

approximately 10% of the load. For the failure of strut S4 for medium clays, substantial load increase percentages for strut S5 are found, reaching approximately 1.5 times of the original strut forces, probably because of the outward movement of the wall into the excavation.

For the 3D analyses, the percentage of the load transfer to adjacent struts and the percentage of the load increase of the relevant struts for medium clay with stiff walls are tabulated in Tables 10 and 11 for $L/B = 2.2$, and in Tables 12 and 13 for $L/B = 3.4$. The tables show that the struts affected most are located directly above or below the failed strut S4 or diagonally across, as plotted in Fig. 4.

When the wall is also stiff, the top strut is able to carry

Table 14 Load transfer percentage from 3D analyses for the one-strut failure of S3 for stiff clay ($L/B = 2.2$)

Struts	Load Transfer %				
	$x = -8$	$x = -4$	$x = 0$	$x = 4$	$x = 8$
stiff clay, $\alpha=0.1$					
S1	-0.5	-3.7	-5.1	0.0	0.0
S2	0.1	4.8	12.6	5.8	1.6
S3	1.4	4.6	Failed strut	5.4	2.6
S4	3.4	6.8	12.3	6.6	7.2
S5	4.5	5.0	4.7	4.8	3.8
stiff clay, $\alpha=1.0$					
S1	0.0	0.8	0.8	0.9	0.1
S2	1.2	4.8	17.9	4.8	1.4
S3	1.3	4.3	Failed strut	4.3	1.5
S4	2.5	6.0	17.5	5.9	2.7
S5	3.8	5.6	6.6	5.6	3.7
stiff clay, $\alpha=10$					
S1	0.1	3.3	7.1	3.3	0.2
S2	0.5	4.2	11.8	4.2	0.6
S3	0.7	4.3	Failed strut	4.3	0.8
S4	1.1	4.2	11.1	4.3	1.2
S5	1.3	3.6	6.5	3.6	1.3

Table 15 Load increase percentage from 3D analyses for the one-strut failure of S3 for stiff clay ($L/B = 2.2$)

Struts	Load increase %				
	$x = -8$	$x = -4$	$x = 0$	$x = 4$	$x = 8$
stiff clay, $\alpha = 0.1$					
S1	0.2	0.1	-2.5	0.1	0.3
S2	1.2	5.5	13.1	5.7	1.4
S3	1.8	4.8	Failed strut	5.4	1.9
S4	2.2	6.9	14.1	6.9	2.2
S5	6.1	9.7	9.9	9.6	6.0
Stiff clay, $\alpha = 1.0$					
S1	0.0	1.6	1.6	1.8	0.3
S2	1.3	5.1	19.2	5.2	1.6
S3	1.3	4.3	Failed strut	4.3	1.5
S4	3.0	7.1	20.6	7.0	3.3
S5	6.1	22.5	26.5	22.5	6.1
Stiff clay, $\alpha = 10$					
S1	0.2	4.2	9.2	4.3	0.3
S2	0.6	4.3	12.2	4.4	0.7
S3	0.7	4.3	Failed strut	4.4	0.8
S4	1.4	5.5	14.3	5.6	1.6
S5	6.0	16.2	28.8	16.1	6.2

The influence of the one-strut failure from 3D analyses for the stiff clay is shown in Fig. 5. The load transfer and load increase percentages for stiff clay are listed in Tables 14 and 15 for $L/B = 2.2$, and Tables 16 and 17 for $L/B = 3.4$.

Table 16 Load transfer percentage from 3D analyses for the one-strut failure of S3 for stiff clay ($L/B = 3.4$)

Struts	Load Transfer %				
	$x = -8$	$x = -4$	$x = 0$	$x = 4$	$x = 8$
stiff clay, $\alpha=0.1$					
S1	-0.5	-3.7	-5.1	0.0	0.0
S2	0.1	4.8	12.6	5.8	1.6
S3	1.4	4.6	Failed strut	5.4	2.6
S4	3.4	6.8	12.3	6.6	7.2
S5	4.5	5.0	4.7	4.8	3.8
stiff clay, $\alpha=1.0$					
S1	-0.2	0.6	0.6	0.8	0.1
S2	1.2	4.6	17.8	4.9	1.6
S3	1.3	4.1	Failed strut	4.4	1.8
S4	3.2	6.0	17.3	6.1	3.0
S5	4.6	5.9	6.6	5.8	4.2
stiff clay, $\alpha = 10$					
S1	-0.3	3.0	5.9	3.1	-0.1
S2	0.7	4.4	12.1	4.5	0.9
S3	1.6	5.0	Failed strut	5.1	1.7
S4	3.0	4.4	11.1	5.9	3.0
S5	4.7	6.6	9.3	6.5	4.4

Table 17 Load increase percentage from 3D analyses for the one-strut failure of S3 for stiff clay ($L/B = 3.4$)

Struts	Load Increase %				
	$x = -8$	$x = -4$	$x = 0$	$x = 4$	$x = 8$
stiff clay, $\alpha = 0.1$					
S1	-0.8	-6.2	-8.7	0.1	0.0
S2	0.1	4.9	12.9	5.9	1.7
S3	1.4	4.6	Failed strut	5.4	2.6
S4	3.7	7.5	13.6	7.3	8.0
S5	14.8	16.4	15.4	15.8	12.4
stiff clay, $\alpha = 1.0$					
S1	-0.4	1.2	1.2	1.6	0.2
S2	1.3	4.9	18.8	5.2	1.7
S3	1.3	4.1	Failed strut	4.5	1.8
S4	3.6	6.7	19.2	6.8	3.4
S5	17.7	22.9	25.6	22.6	16.3
stiff clay, $\alpha = 10$					
S1	-0.4	3.8	7.6	4.0	-0.1
S2	0.7	4.5	12.4	4.6	0.9
S3	1.6	5.0	Failed strut	5.2	1.7
S4	3.8	5.4	13.7	7.5	3.8
S5	23.1	32.7	46.0	32.5	22.0

The load is mainly transferred to the struts directly above and below the failed strut S3, and the load transfer percentage is approximately 10% to 20%. Apart from these two struts, the struts at the bottom level S5 are also

subjected to quite a high load transfer percentage increase of approximately 30% for the medium and stiff walls. However, in terms of the load increase percentage, for stiff clays the increases are significantly smaller than for the soft and medium clays.

The 3D results again highlight that the 2D analyses would result in fairly conservative (i.e., larger) estimates of the loads transferred to the adjacent struts from the failed strut as it ignores the restraining effects of the adjacent horizontal struts.

4. Conclusions

In this paper, the finite element simulation of one-strut failure of multi-level braced excavations was considered. The 3D one-strut failure analysis indicates that the 2D analyses would result in fairly conservative (i.e., larger) estimates of the loads transferred to the adjacent struts from the failed strut as it ignores the restraining effects of the adjacent horizontal struts. Therefore, 2D analysis would result in a more conservative design. This may result in a larger strut size and larger waler size which would increase costs.

Acknowledgements

The corresponding author is grateful to the support by the National Natural Science Foundation of China (No. 51608071), the Advanced Interdisciplinary Special Cultivation program of Chongqing University (No. 106112017CDJQJ208850), and Key Laboratory of Rock Mechanics in Hydraulic Structural Engineering, Ministry of Education, Wuhan University (No. RMHSE1601).

References

- Brinkgreve, L.B.J., Swolfs, W.M. and Engin, E. (2011), *Plaxis Manual*, PLAXIS, The Netherlands.
- Bryson, L.S. and Zapata-Medina, D.G. (2012), "Method for estimating system stiffness for excavation support walls", *J. Geotech. Geoenviron. Eng.*, **138**(9), 1104-1115.
- Chang, J.D. and Wong, K.S. (1997), "Apparent pressure diagram for braced excavation in soft clay with diaphragm wall", *Proceedings of the International Symposium on Geotechnical Aspects of Underground Construction in Soft Ground*, London, U.K.
- Endicott, J. (2013), "Case histories of deep excavation. Examination of where things went wrong: Nicoll Highway Collapse, Singapore", *Proceedings of the International Conference on Case Histories in Geotechnical Engineering*, Chicago, Illinois, U.S.A., April.
- Finno, R.J., Blackburn, J.T. and Roboski, J.F. (2007), "Three-dimensional effects for supported excavations in clay", *J. Geotech. Geoenviron. Eng.*, **133**(1), 30-36.
- Finno, R.J., Bryson, S. and Calvello, M. (2002), "Performance of a stiff support system in soft clay", *J. Geotech. Geoenviron. Eng.*, **128**(8), 660-671.
- Goh, A.T.C., Zhang, Y., Zhang, R., Zhang, W. and Xiao, Y. (2017), "Evaluating stability of underground entry-type excavations using multivariate adaptive regression splines and logistic regression", *Tunn. Undergr. Sp. Technol.*, **70**, 148-154.
- Goh, A.T.C. and Wong, K.S. (2009), "Three-dimensional analysis of strut failure for braced excavation in clay", *J. Southeast Asian Geotech. Soc.*, **40**(2), 137-143.
- Hashash, Y.M. and Whittle, A.J. (2002), "Mechanisms of load transfer and arching for braced excavations in clay", *J. Geotech. Geoenviron. Eng.*, **128**(3), 187-197.
- Hsieh, P.G. and Ou, C.Y. (1998), "Shape of ground surface settlement profiles caused by excavation", *Can. Geotech. J.*, **35**(6), 1004-1017.
- Liao, S.S. and Neff, T.L. (1990), "Estimating lateral earth pressures for design of excavation support", *Proceedings of the Specialty Conference on Design and Performance of Earth Retaining Structures*, New York, U.S.A., June.
- Long M. (2001), "Database for retaining wall and ground movements due to deep excavations", *J. Geotech. Geoenviron. Eng.*, **127**(3), 203-224.
- Low, Y.S., Ng, D.C.C., Chin, Y.Y. and Ting, S.E. (2012), "A Singapore case history of temporary removable ground anchor design to TR26: 2010", *IES J. Part A Civ. Struct. Eng.*, **5**(3), 181-194.
- Moormann, C. (2004), "Analysis of wall and ground movements due to deep excavations in soft soil based on a new worldwide database", *Soil. Found.*, **44**(1), 87-98.
- Ng, C.W.W. (1992), "An evaluation of soil-structure interaction associated with a multi-propped excavation", Ph.D. Dissertation, University of Bristol, Bristol, U.K.
- Ng, C.W.W. and Yan, R.W. (1998), "Stress transfer and deformation mechanisms around a diaphragm wall panel", *J. Geotech. Geoenviron. Eng.*, **124**(7), 638-648.
- Ou, C.Y., Liao, J.T. and Lin, H.D. (1998), "Performance of diaphragm wall constructed using top-down method", *J. Geotech. Geoenviron. Eng.*, **124**(9), 798-808.
- Peck, R.B. (1969), "Deep excavation and tunnelling in soft ground", *Proceedings of the 7th International Conference on Soil Mechanics and Foundation Engineering*, Mexico City, Mexico.
- Pong, K.F., Foo, S.L., Chinnaswamy, C.G., Ng, C.C.D. and Chow, W.L. (2012), "Design considerations for one-strut failure according to TR26-a practical approach for practising engineers", *IES J. Part A Civ. Struct. Eng.*, **5**(3), 166-180.
- Saleem, M. (2015), "Application of numerical simulation for the analysis and interpretation of pile-anchor system failure", *Geomech. Eng.*, **9**(6), 689-707.
- Stille, H. (1976), "Behaviour of anchored sheet pile walls", Ph.D. Dissertation, Royal Institute of Technology, Stockholm, Sweden.
- Stille, H. and Broms, B.B. (1976), "Load redistribution caused by anchor failures in sheet pile walls", *Proceedings of the 6th European Conference on Soil Mechanics and Foundation Engineering*, Vienna, Austria, March.
- TR26 (2010), *Technical Reference for Deep Excavation*, Spring Singapore, Singapore.
- Twine, D. and Roscoe, H. (1997), *Prop Loads: Guidance on Design, CIRIA Core Programme Funders' Report FR/CP/48*, Construction Industry Research and Information Association, London, U.K.
- Van Langen, H. (1991), "Numerical Analysis of Soil-structure Interaction", Ph.D. Dissertation, Delft University of Technology, Delft, The Netherlands.
- Xiang, Y., Goh, A.T.C., Zhang, W. and Zhang, R. (2018), "A multivariate adaptive regression splines model for estimation of maximum wall deflections induced by braced excavation in clays", *Geomech. Eng.*, **14**(4), 315-324.
- Zhang, W.G., Goh, A.T.C., Goh, K.H., Chew, O.Y.S., Zhou, D. and Zhang, R. (2018), "Performance of braced excavation in

residual soil with groundwater drawdown”, *Undergr. Sp.*, **3**,
150-165.

CC